

Nonautonomous Roles of MAB-5/Hox and the Secreted Basement Membrane Molecule SPON-1/F-Spondin in *Caenorhabditis elegans* Neuronal Migration

Matthew P. Josephson, Adam M. Miltner, and Erik A. Lundquist¹

Department of Molecular Biosciences, Programs in Genetics and Molecular, Cellular, and Developmental Biology, University of Kansas, Lawrence, Kansas 66045

ORCID ID: 0000-0001-6819-4815 (E.A.L.)

ABSTRACT Nervous system development and circuit formation requires neurons to migrate from their birthplaces to specific destinations. Migrating neurons detect extracellular cues that provide guidance information. In *Caenorhabditis elegans*, the Q right (QR) and Q left (QL) neuroblast descendants migrate long distances in opposite directions. The Hox gene *lin-39* cell autonomously promotes anterior QR descendant migration, and *mab-5/Hox* cell autonomously promotes posterior QL descendant migration. Here we describe a nonautonomous role of *mab-5* in regulating both QR and QL descendant migrations, a role masked by redundancy with *lin-39*. A third Hox gene, *egl-5/Abdominal-B*, also likely nonautonomously regulates Q descendant migrations. In the *lin-39 mab-5 egl-5* triple mutant, little if any QR and QL descendant migration occurs. In addition to well-described roles of *lin-39* and *mab-5* in the Q descendants, our results suggest that *lin-39*, *mab-5*, and *egl-5* might also pattern the posterior region of the animal for Q descendant migration. Previous studies showed that the *spon-1* gene might be a target of MAB-5 in Q descendant migration. *spon-1* encodes a secreted basement membrane molecule similar to vertebrate F-spondin. Here we show that *spon-1* acts nonautonomously to control Q descendant migration, and might function as a permissive rather than instructive signal for cell migration. We find that increased levels of MAB-5 in body wall muscle (BWM) can drive the *spon-1* promoter adjacent to the Q cells, and loss of *spon-1* suppresses *mab-5* gain of function. Thus, MAB-5 might nonautonomously control Q descendant migrations by patterning the posterior region of the animal to which Q cells respond. *spon-1* expression from BWMs might be part of the posterior patterning necessary for directed Q descendant migration.

KEYWORDS Hox; *mab-5*; *egl-5*; F-spondin; cell migration

HOX transcription factors are principal regulators of cell fate and control major aspects of development, including nervous system development. Hox factors regulate nervous system development in part through cell-autonomous specification of cell fate, axon guidance, and regulation of migratory neural progenitors (Studer *et al.* 1996; Gavalas *et al.* 1997; Arenkiel *et al.* 2004). Additionally there is evidence that Hox genes in the developing brain can cell nonautonomously control axon guidance (Gavalas *et al.* 1997). Neuron

migration is an important aspect of nervous system development and many neurons and neuroblasts migrate from their initial birthplace to specific regions of the periphery (neural crest) or cortex. The Q neuroblasts of *Caenorhabditis elegans* represent a tractable and well-studied model for Hox gene-controlled neuroblast migration (Chapman *et al.* 2008; Middelkoop and Korswagen 2014). The Q neuroblasts Q right (QR) and Q left (QL) are bilaterally symmetric cells that undergo identical patterns of division, migration, and apoptosis to produce three neurons each (Sulston and Horvitz 1977). QR on the right side of the animal migrates anteriorly, undergoing cell division and migration, giving rise to three neurons, with AQR migrating the farthest residing near the posterior pharyngeal bulb (Sulston and Horvitz 1977; Chapman *et al.* 2008). QL migrates posteriorly undergoing

Copyright © 2016 by the Genetics Society of America
doi: 10.1534/genetics.116.188367

Manuscript received February 18, 2016; accepted for publication May 20, 2016; published Early Online May 24, 2016.

¹Corresponding author: 1200 Sunnyside Ave., 5049 Haworth Hall, University of Kansas, Lawrence, KS 66045. E-mail: erikl@ku.edu

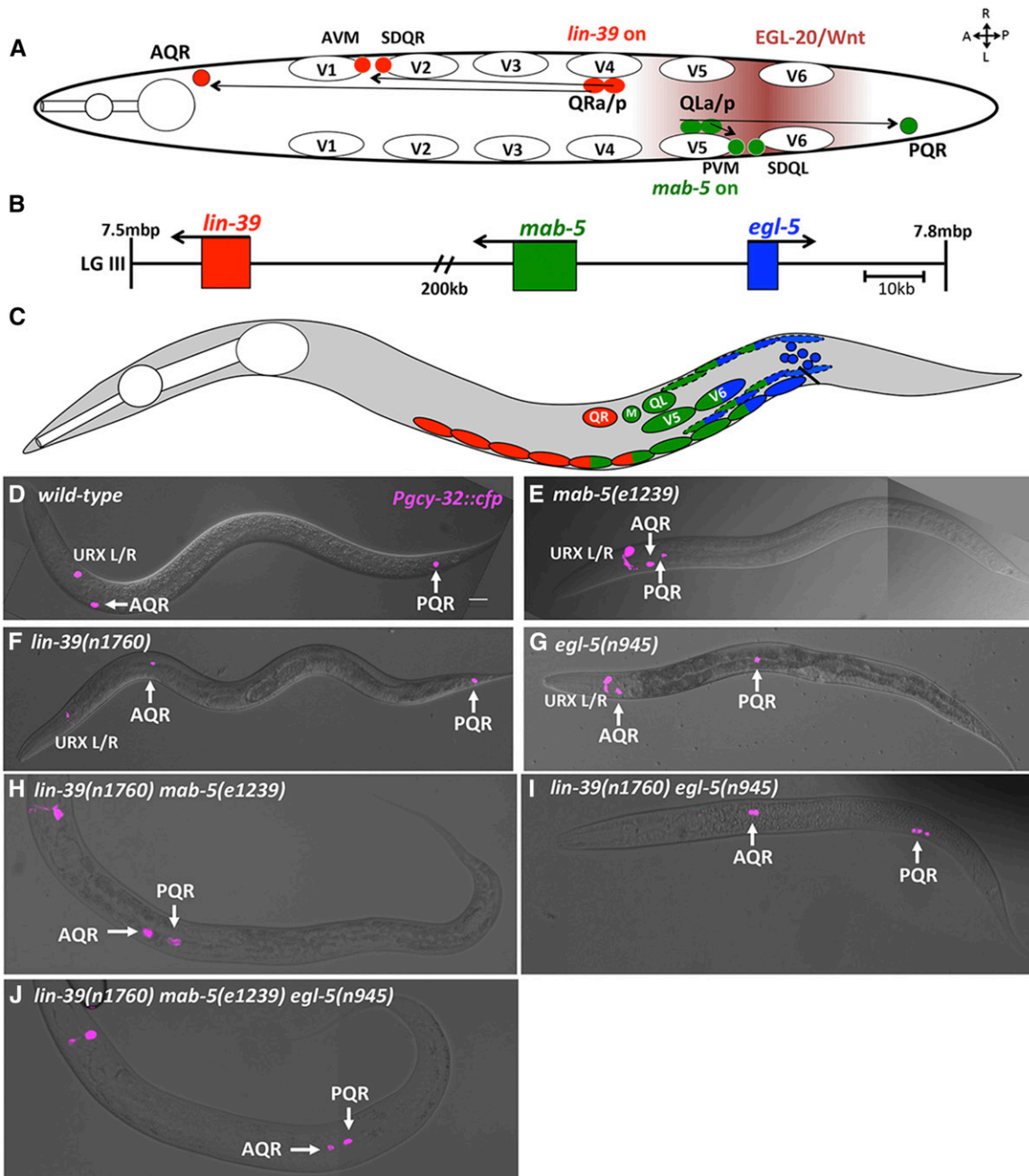


Figure 1 *C. elegans* Hox genes *lin-39*, *mab-5*, and *egl-5* affect Q descendant migrations. (A) Diagram of a dorsal view of wild-type Q descendant migration. EGL-20/Wnt (maroon shading) induces MAB-5 in QL and descendants, which directs posterior migration. QR and descendants do not respond to EGL-20/Wnt, and express *lin-39*, driving anterior migration. (B) Position on LGIII (7.5–7.8 Mbp) of the three *C. elegans* Hox genes that effect postembryonic development. (C) representation of cells that express *lin-39* (red), *mab-5* (green), and *egl-5* (blue) during the L1 larval stage. Dashed ovals represent BWMs, solid ovals the P cells, and blue circular cells near the anus represent the rectal epithelium where *egl-5* is expressed. (D–J) Positions of Q descendants AQR and PQR in L4/young adult animals. *lqls58*[*Pgcy-32::cfp*] micrographs were merged with DIC micrographs in wild-type and mutants. In all micrographs unless otherwise noted, dorsal is up, anterior is left. Bar, 10 μ m.

identical cell divisions, giving rise to three neurons, of which PQR migrates the farthest to reside posterior to the anus, near the phasmid ganglion (Chalfie *et al.* 1983; Kenyon 1986; Salser and Kenyon 1992; Whangbo and Kenyon 1999; Korswagen *et al.* 2000; Chapman *et al.* 2008).

Hox transcription factors govern QR and QL descendant migrations. Canonical Wnt signaling through detection of

extracellular EGL-20/Wnt induces transcription of *antennapedia*-like Hox gene *mab-5* in the Q cells (Maloof *et al.* 1999). MAB-5 is necessary in the QL lineage for posterior migration, and in the absence of MAB-5 all QL daughters migrate anteriorly (Harris *et al.* 1996). MAB-5 is also sufficient for posterior Q cell migrations, as expression of MAB-5 in QR causes posterior migration of the entire QR lineage (Salser and

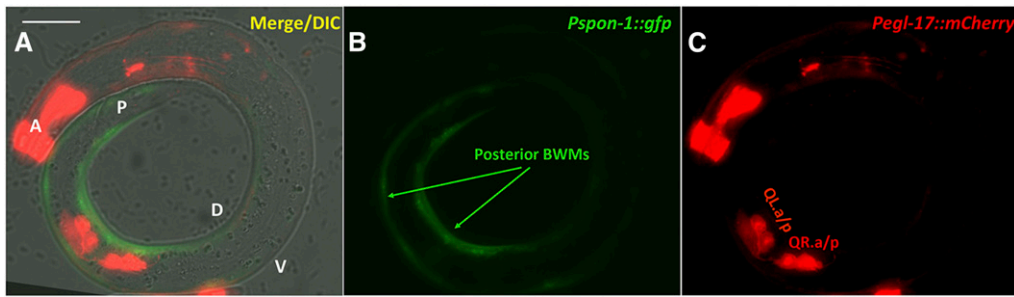


Figure 3 *Pspn-1::gfp* expression. Micrographs of an L1 larva at 4–4.5 hr posthatching are shown. (A) *Pspn-1::gfp* expression in posterior BWMs. (B) Qx.a/p visualized using *rdvls1[Pegl-17::mCherry]*. (C) Merged *Pspn-1::gfp*, *Pegl-17::mCherry*, and DIC images. The animal is coiled such that the anterior (A) is near the posterior (P). Dorsal (D) and ventral (V) are indicated. Bar, 10 μ m.

we describe AQR and PQR migration defects in *egl-5* mutants, expression of which is not detectable in Q lineages. Together, these results point to a nonautonomous role of *mab-5* and possibly *lin-39* and *egl-5* in Q migrations. Expression of these genes might pattern the posterior of the animal, providing migration information to the Q descendants. Thus, *MAB-5* and *LIN-39* might both establish an anterior–posterior Q descendant guidance system (nonautonomous role) and control how the Q descendants respond to this guidance system (autonomous role).

A previous RNA-seq study identified *spn-1* as a potential transcriptional target of *MAB-5* (Tamayo *et al.* 2013). The *mab-5(e1751)* gain-of-function (*gof*) mutation causes ectopic expression of *mab-5* in many cells, including QR, and drives posterior migration of the QR descendant AQR (Salser *et al.* 1993; Chapman *et al.* 2008). RNA-mediated interference (RNAi) knockdown of *spn-1* partially suppressed posterior AQR migration in *mab-5(gof)*, suggesting that *spn-1* mediates the effects of *mab-5(gof)* in posterior migration (Tamayo *et al.* 2013). *spn-1* encodes a secreted basement membrane molecule similar to vertebrate F-spondin (Woo *et al.* 2008). In vertebrates, F-spondin is secreted by the floor plate of the neural tube and has multiple roles in neural adhesion, neural crest migration, and axon guidance (Klar *et al.* 1992; Burstyn-Cohen *et al.* 1999; Debby-Brafman *et al.* 1999; Zisman *et al.* 2007). F-spondin becomes processed into three peptides that can both attract and repel developing axons (Tzarfaty-Majar *et al.* 2001; Zisman *et al.* 2007). F-spondin has been implicated in Alzheimer's disease (AD) as a binding partner to amyloid precursor protein, with F-spondin treatment improving memory and β -amyloid levels in AD model mice (Ho and Sudhof 2004; Hoe *et al.* 2005; Hafez *et al.* 2012). In addition to its role in disease, F-spondin is conserved in many species, including and has domain similarity to the established nervous system development molecule Reeler (Klar *et al.* 1992; Higashijima *et al.* 1997; Burstyn-Cohen *et al.* 1999; Hu *et al.* 2016). In *C. elegans*, *SPON-1*/F-spondin plays a role in neural adhesion and development (Woo *et al.* 2008). *spn-1* is required for muscle cell adhesion, and null or strong loss-of-function mutants are embryonic lethal (Woo *et al.* 2008). Despite being an important nervous system development molecule, little is known about the regulation of F-spondin expression. Here we show that *spn-1* itself is required for AQR and PQR migration. Furthermore, we show that *spn-1* promoter activity in BWMs can be driven by *MAB-5*, and that *spn-1* phenotypes are rescued by

BWM-derived *SPON-1*. Finally, we present evidence that *spn-1* acts in BWM to mediate the effects of *mab-5(gof)*. Taken together, our results suggest that *mab-5* has a nonautonomous role in Q descendant migration, possibly by patterning the posterior region of the animal for proper Q migration. Further, they suggest that the *spn-1*/*F-spondin* gene might be a target of *MAB-5* in posterior BWMs, which in part provides information for Q descendant migration.

Materials and Methods

Genetics

All experiments were carried out using standard *C. elegans* technique at 20°C (Brenner, 1974). Mutations used were: LGX: *qls2*[*Posm-6::gfp*]; LGI: *lrp-1(ku156)*. LGII: *spn-1(e2623, ju430ts, ju402)*, *hlh-1(cc561)*, *muIs16[mab-5::gfp]*. LGIII: *mab-5(e1239, e2088, e1751)*, *lin-39(n1760)*, *egl-5(n945)*, *rdvls1[Pegl-17::mCherry]*. LGIV: *qls80* [*Pscm::gfp::caax*]. LGV: *sid-1(pk3321)*, *qls58*[*Pgcy-32::cfp*], *wgIs54* [*egl-5::TY1::egfp::3xFLAG, UNC-119+*]. Unknown chromosomal location, *qls227* and *qls228* [*Pspn-1::gfp*], and *qls271*[*Pmyo-3::mab-5*]. *qls227* and *qls228* were created by integration of *juEx592* (Woo *et al.*, 2008), and *qls271* by integration of *lqEx808*. Extrachromosomal arrays were generated using standard gonadal injection (Mello and Fire, 1995) and include: *lqEx708* and *lqEx709* [*Pscm::spn-1(RNAi), Pgcy-32::cfp*]; *lqEx732* and *lqEx937* [*Pegl-17::spn-1(RNAi), Pgcy-32::cfp*]; *lqEx808* [*Pmyo-3::mab-5, Pgcy-32::cfp*]; *lqEx834* [*Pegl-17::myr-mCherry, Pegl-17::mCherry::HIS-24*]; *lqEx849* [*Pegl-17::REELER, Pgcy-32::yfp*]; *lqEx854* [*Pegl-17::REELER::gfp, Pgcy-32::cfp*]; *lqEx855, lqEx856* and *lqEx858* [*Pegl-17::TSR1-5, Pgcy-32::cfp*]; *lqEx859* and *lqEx860* [*Pmyo-3::spn-1, Pgcy-32::cfp*]; *lqEx897* and *lqEx898* [*Pspn-1::mab-5::cfp, Pgcy-32::yfp*]; *lqEx759* [*Pegl-17::spn-1*]; *lqEx938, lqEx940* and *lqEx941* [*Pmyo-3::spn-1(RNAi), Pscm::gfp, Pgcy-32::mCherry*]; *lqEx942* [*Pgcy-32::yfp*], into *lin-39(n1760)* *egl-5(n945)*; *lqEx930* and *lqEx943* [*Pspn-1::EGL-5::cfp, Pgcy-32::yfp*].

Transgene construction

Details about transgene construction are available by request. The entire *spn-1* genomic region was amplified by PCR and placed behind *myo-3* and *egl-17* promoters. *Pegl-17::SP::TSR1-5* contained the *spn-1* endogenous signal peptide, first 29 residues, followed by the five thrombospondin repeats, residues

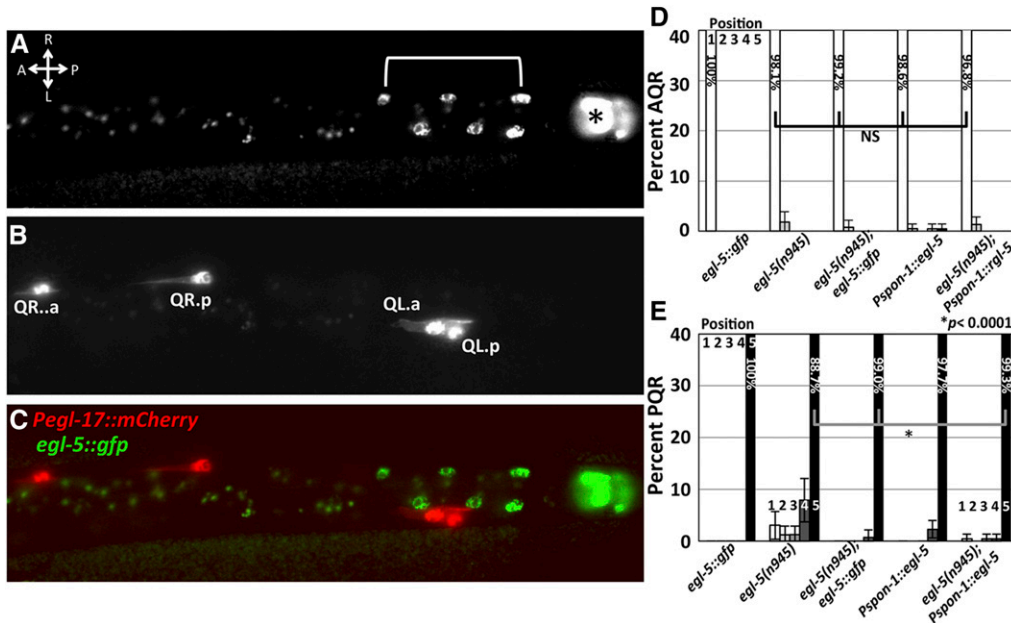


Figure 4 Full-length *egl-5::gfp* expression. Fluorescent micrographs of posterior region of an L1 larva at 5–5.5 hr posthatching, dorsal view. Anterior is left. Bar, 5 μ m. (A) *egl-5::gfp* (*wgl54*). The asterisk indicates rectal epithelial expression of *egl-5::gfp*, and brackets indicate nuclei of posterior BWMs or P cells. The punctate fluorescence anterior to the bracketed nuclei is background autofluorescence of the gut. (B) *Pegl-17::mCherry*. (C) Merged image. (D and E) *egl-5::gfp* and *Pspn-1::egl-5* transgenic rescue of *egl-5(n945)* as described for Figure 2. Combined results of two independent *Pspn-1::egl-5* arrays that showed similar effects are shown.

431–819. *Pegl-17::Reeler* was made by using the first 430 residues, which contain both the Reeler and Spondin domains. *Pmyo-3::mab-5* was using a *mab-5* complementary DNA with the first endogenous *mab-5* intron (the *mab-5* minigene). *Pspn-1::mab-5::cfp* was made fusing the *mab-5* minigene to *cfp* at the C terminus. *Pspn-1::egl-5::cfp* was made using the entire *egl-5* genomic region.

Scoring AQR and PQR migration

Scoring was done using *Pgcy-32*, which is expressed exclusively in AQR, PQR, and URX1/r (Chapman *et al.* 2008). The position of AQR and PQR was scored as previously described using a compound fluorescent microscope (Chapman *et al.* 2008; Dyer *et al.* 2010). *ju430ts* animals were allowed to lay eggs for 3 hr at 15°, then plates were shifted to 20°. Some animals exhibited *pat* phenotype; viable animals were scored for AQR and PQR as described above. The triple mutant *lin-39 mab-5 egl-5* was maintained over the *hT2* balancer, and scored progeny had wild-type maternal contribution for each gene. Some *Hox* single and double mutant combinations were balanced by *hT2*. Positions 4a and 4b were separated by the PDE neuron marked by *Posm-6::gfp*, which represents the region of Q cell birth. Neurons directly over the PDE were marked as position 4a. Significance of difference was determined by Fisher's exact test.

Line scan analysis of *Pspn-1::gfp* expression

Animals were synchronized to 4–4.5 hr posthatching using previous published techniques (Honigberg and Kenyon 2000; Chapman *et al.* 2008). Animals were mounted on a 2% (w/v) agarose pad in M9 containing 5 mM sodium azide. Fluorescent micrographs were acquired for 100 ms at $\times 100$ using a Qimaging Rolera EM CCD camera and Metamorph software. Intensity of GFP was measured using ImageJ. Lines were drawn 1 pixel wide from the center of the posterior pharyngeal bulb to the posterior end of the anus on both dorsal and

ventral BWM segments. Segmented lines were drawn through BWM nuclei, with pixels set at the anterior, posterior, and center of each muscle cell. Only animals that had both left and right muscle quadrants aligned were scored. To account for animal curvature, we averaged pixel intensity over each percentage of each line measured. This gives a percentage referring to the percentage of distance from anterior to posterior of the animal. This gave similar results to artificial straightening using ImageJ and was less cumbersome. Twenty animals were imaged on both dorsal and ventral segments for each genotype, yielding 40 scans per genotype. In our analysis, dorsal and ventral data were combined for each animal, and any dorsal–ventral differences were not included. Standard deviations were calculated for each percentage position (error bars), and a two-tailed Student's *t*-test with unequal variance was used to determine significance of difference at each percentage position using a Bonferroni correction for multiple comparisons (100 in each genotype, $Q < 0.05$, $P < 0.0005$). Transgenes *lqls227* and *lqls228* showed similar posterior bias and *lqls227* was chosen for subsequent analysis due to chromosomal location (*lqls227* is on the region of LGI balanced by *hT2*). For *lin-39 mab-5 egl-5* triple hox line scan analysis, *lqls228* was used for comparison, due to linkage of the *lqls227* transgene.

Data availability

The authors state that all data necessary for confirming the conclusions presented in the article are represented fully within the article.

Results

Hox genes *mab-5*, *lin-39*, and *egl-5* control QR and QL descendant migrations

The bilateral neuroblasts QR and QL, born in the posterior between the vulva and anus, give rise to the AQR and PQR

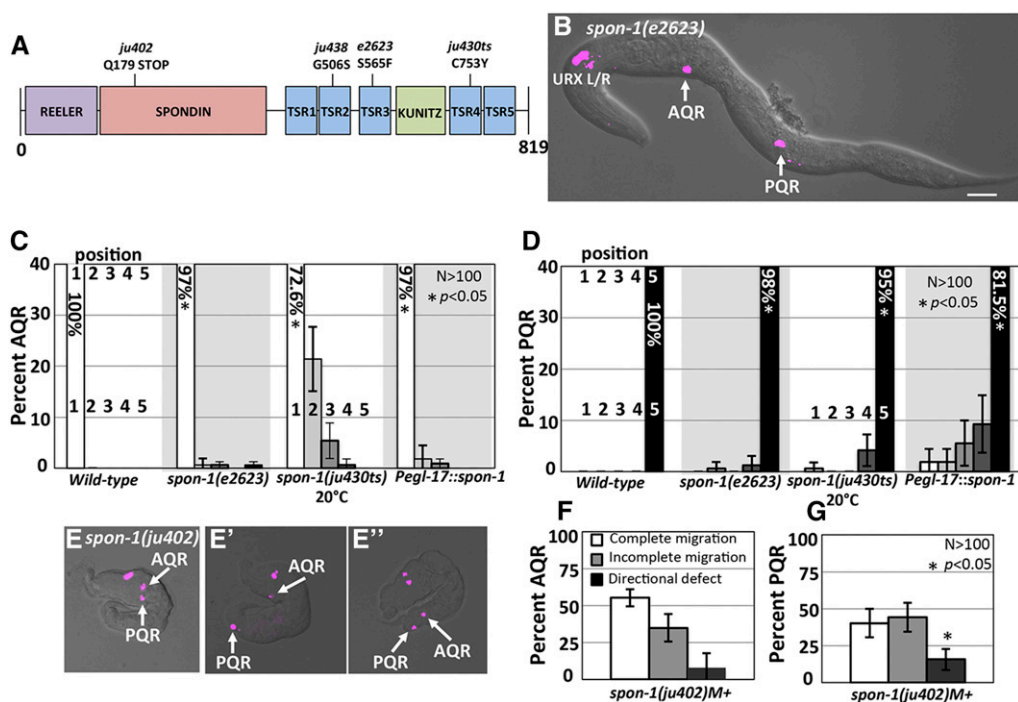


Figure 5 AQR and PQR migration defects in *spn-1* mutants. (A) Diagram of the predicted 819-residue SPON-1 molecule with Reeler, Spondin, Thrombospondin (TSR), and Kunitz serine protease inhibitor (KUNITZ) domains shown. The positions of mutations are indicated. (B) A *spn-1(e2623)* young adult animal with defects in AQR and PQR migration (merged *cfp* and DIC micrographs). Bar, 20 μ m. (C and D) AQR and PQR migration defects in *spn-1* as described in Figure 2. Error bars represent 2 \times standard error of the proportion. (E–E'') *spn-1(ju402)M+* arrested L1 animals with *Pgcy-32::cfp*. (E) PQR reversal in migration direction. (E') Complete AQR and PQR migration. (E'') AQR directional defect. (F and G) Percent of AQR (F), and PQR (G) that show defects in *spn-1(ju402)M+*-arrested L1 animals.

neurons, respectively (Sulston and Horvitz 1977) (Figure 1A). In *wild-type* animals, AQR migrates anteriorly to a region near the anterior deirid, and PQR migrates posteriorly to a position posterior to the anus in the phasmid ganglion (White *et al.* 1986; Chapman *et al.* 2008) (Figure 1A). The Hox transcription factors *lin-39*, *mab-5*, and *egl-5* are expressed in specific regions ranging from anterior to posterior and resemble a Hox cluster on chromosome III (Kenyon 1986; Chisholm 1991; Clark *et al.* 1993; Salser *et al.* 1993; Wang *et al.* 1993; Van Auken *et al.* 2000) (Figure 1, B and C). *MAB-5* is required in QL to direct QL descendant migrations including PQR (Salser and Kenyon 1992) (Figure 1, A and E). *LIN-39* has been shown to cell-autonomously promote anterior migration of QR descendants, and *lin-39* is normally inhibited by *MAB-5* in QL.a/p to allow for posterior migration (Figure 1, A and F) (Harris *et al.* 1996; Wang *et al.* 2013).

We scored AQR and PQR position using *Pgcy-32::cfp* along five positions in the animal as previously described (see *Materials and Methods* and Figure 2A) (Chapman *et al.* 2008). As expected, *lin-39* mutants showed shortened anterior migration of the QR descendant AQR (Figure 1F and Figure 2B). *lin-39* displayed minor (4%), but significant defects in PQR migration (Figure 2C). *mab-5* mutants affected only PQR migration, with 100% of PQR misdirected, mostly residing in the normal anterior position of AQR (Figure 1E and Figure 2, B and C). *egl-5* mutants were reported to have weak QL defects (Desai and Horvitz 1989; Chisholm 1991). We found that *egl-5* affected both AQR and PQR migration: 2% of AQR failed to migrate fully and 16% of PQR failed to migrate, or migrated anteriorly (Figure 1G and Figure 2, B and C).

Previous studies found that *lin-39* and *mab-5* act in parallel in QR descendant migration (Clark *et al.* 1993; Wang *et al.*

1993). In a *lin-39 mab-5* double mutant, AQR migration defects were significantly stronger compared to *lin-39* alone, and misdirected PQRs failed in their anterior migration (Figure 1H and Figure 2, B and C). These data suggest that *MAB-5* acts in parallel with *LIN-39* in anterior migration.

mab-5 egl-5 double mutants showed no significant difference in AQR migration from *egl-5* alone (Figure 2B). Most PQR were directed anteriorly in the *mab-5 egl-5* double, but some failed in their anterior migration, consistent with the weak anterior AQR migration defects in *egl-5* single mutants. *lin-39 egl-5* double mutants had AQR defects similar to an additive effect of *lin-39* and *egl-5* single mutants (Figure 1I and Figure 2, B and C). PQR defects in *lin-39 egl-5* animals were significantly increased compared to an additive effect of both single mutants, suggesting they act in parallel (Figure 2, B and C). Similarly, the *lin-39 mab-5 egl-5* triple mutant showed significantly more severe AQR and PQR migration defects compared to any double *Hox* mutant (Figure 1J and Figure 2, B and C). Most AQR and PQR remained near their birth positions with minimal anterior or posterior migration. These results suggest that *lin-39*, *mab-5*, and *egl-5* are required in parallel for both anterior and posterior migration of QL and QR descendants AQR and PQR, and in their absence, very little migration occurs.

mab-5 and *egl-5* can act in BWM to control AQR and PQR migration

These data suggest that the Hox genes *LIN-39*, *MAB-5*, and *EGL-5* act in parallel pathways to promote both anterior and posterior migration of QR and QL descendants AQR and PQR. *mab-5* is not expressed in QR descendants (Salser *et al.* 1993; Harris *et al.* 1996; Salser and Kenyon 1996), and *lin-39*

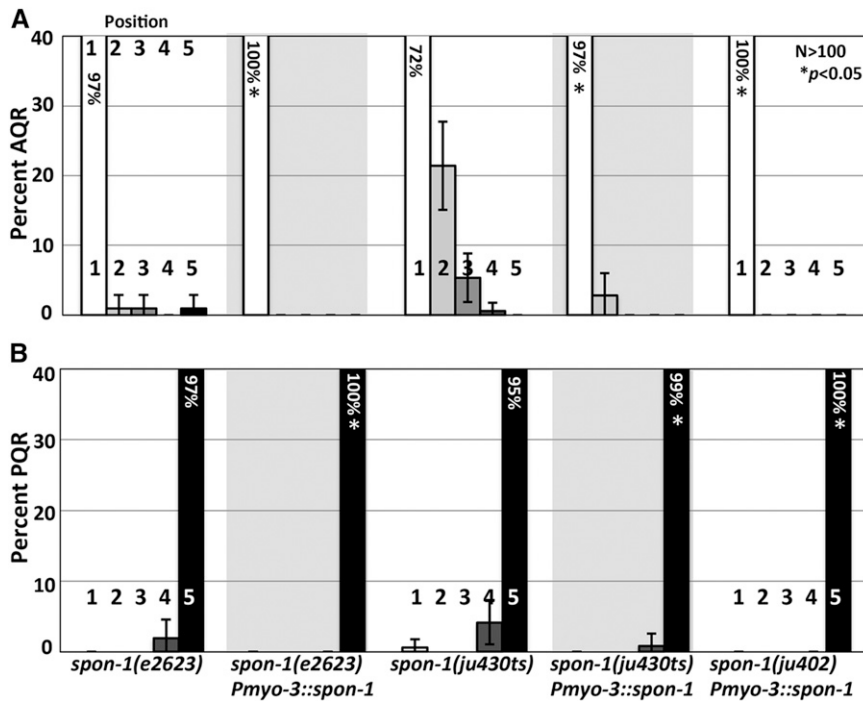


Figure 6 Muscle-derived SPON-1 rescues AQR and PQR migration. (A and B) Quantification of AQR (A) and PQR (B) positions as in Figure 2. *Pmyo-3::spn-1* represents the transgene expressing SPON-1 in BWM cells. Asterisk indicates significant ($n > 100$, $P < 0.05$ Fisher's exact test) difference from corresponding *spn-1* mutant (except for *ju402*, which is lethal). Data for transgenic arrays are the combined results from two independently derived arrays with similar effects.

autonomously drives anterior QR descendant migration and is repressed in QL by *mab-5* (Harris *et al.* 1996; Wang *et al.* 2013). However, both are expressed in other posterior cells, including P cells, and MAB-5 in posterior BWMs and seam cells (Salser *et al.* 1993; Wang *et al.* 1993; Clandinin *et al.* 1997; Maloof *et al.* 1999; Yang *et al.* 2005; Wagmaister *et al.* 2006a,b) (Figure 1C). Thus, the effects of *mab-5* on AQR migration and *lin-39* on PQR migration might be due to their roles in cells other than Q descendants. However *lin-39* is expressed briefly in QL lineage, which could be important for initial migration (Wang *et al.* 1993).

MAB-5 is expressed in posterior BWMs (Salser *et al.* 1993) (Figure 1C). We drove expression of MAB-5 specifically in BWMs using the promoter of the *spn-1* gene (Woo *et al.* 2008). At the time of Q descendant migration, *Pspn-1::gfp* was expressed most strongly in posterior BWMs in the region of the Q cells, but not in the Q cells themselves (Figure 3). *Pspn-1::mab-5* significantly rescued the AQR and PQR defects seen in the *lin-39 mab-5* double mutant [e.g., 4–44% of AQR in position 1, and 2–19% of PQR in position 1 ($P < 0.05$)] (Figure 2, B and C). These results show that MAB-5 can have a role in AQR and PQR migration through activity in BWMs. Importantly, direction of PQR migration was not rescued by *Pspn-1::mab-5* (e.g., PQRs still migrated anteriorly). Direction of migration is an established cell-autonomous role of *mab-5* and not expected to be rescued by muscle-specific *Pspn-1::mab-5*. This also shows that *Pspn-1::mab-5* did not lead to expression of *mab-5* in the Q descendants, as transgenic expression of *mab-5* in Q descendants leads to posterior migration of AQR and PQR (Josephson *et al.* 2016). These data argue that *mab-5* has a nonautonomous role in anterior AQR and PQR migration.

egl-5 is expressed in posterior cells, but not in the Q cells (Ferreira *et al.* 1999). We examined expression of the full-length *egl-5::gfp(wgIs54)* transgene from the modENCODE project (Niu *et al.* 2011). This transgene rescued PQR migration defects of *egl-5(n945)* (Figure 4), but showed no detectable expression in the Q cells. *egl-5::gfp* was expressed in other posterior cells, consistent with previously described expression (Figure 4) (Ferreira *et al.* 1999). Similar to above, we tested the nonautonomous role of EGL-5 by expressing it from the *spn-1* promoter. *Pspn-1::egl-5::cfp* weakly effected PQR migration on its own and rescued the stronger PQR migration defects of *egl-5* (Figure 4) but did not rescue the coiler phenotype of *egl-5* (data not shown). These data are consistent with a nonautonomous role of EGL-5 in Q descendant migration, likely in posterior BWM.

SPON-1 is required for proper Q descendant migration

Potential MAB-5 transcriptional targets in Q descendant migration were identified previously by whole-animal RNA-seq on *wild-type* and *mab-5* mutants coupled with functional suppression of *mab-5(e1751)* *gof* (Tamayo *et al.* 2013). *spn-1* transcripts were over-represented in *mab-5(gof)*, and reduction of *spn-1* function partially suppressed posterior AQR migration in *mab-5(gof)* (Tamayo *et al.* 2013). These results indicate that *spn-1* expression is regulated by MAB-5 and that SPON-1 is required for posterior AQR migration in *mab-5(gof)*. *spn-1* encodes a molecule similar to vertebrate F-spondin, a secreted basement membrane molecule, and is required for proper muscle cell attachment and neural development (Woo *et al.* 2008) (Figure 5A).

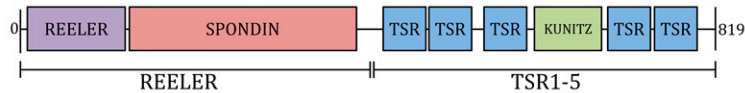
spn-1 null mutation results in embryonic lethality due to muscle cell detachment (Woo *et al.* 2008). We first used the

Table 1 *mab-5* and *spn-1* ectopic expression

Table 1. *mab-5* and *spn-1* ectopic expression.

Genotype	AQR position (%)						PQR position (%)					
	1	2	3	4	5	N	1	2	3	4	5	N
<i>wildtype</i>	100	0	0	0	0	300	0	0	0	0	100	300
<i>Pegl-17::spn-1</i>	99	1	0	0	0	108	2	2	6	9	81*	108
<i>Pegl-17::SP::TSR1-5</i>	99.5*	0.25	0	0	0.25	386	0.3	0	0	0.5	99.2*	372
<i>Pegl-17::Reeler/spndin</i>	99.5*	0	0	0	0.5	216	0.5	0	0.5	3	96*	265
<i>Pmyo-3::mab-5</i>	97*	3	0	0	0	210	0	0	0	0	100	210
<i>Pspn-1::mab-5</i>	99*	0.3	0.3	0.3	0	277	0	0	0	0	100	277
<i>Pmyo-3::spn-1</i>	99*	0	0.5	0.5	0	289	0	0	0	0	100	303
<i>Pmyo-3::spn-1(RNAi)</i>	99*	1	0	0	0	364	0	0	0	0	100	364

* $p < 0.05$ compared to wildtype



Animals were scored with *Pgcy-32::cfp* marking AQR and PQR. All genotypes with transgenes except *Pmyo-3::mab-5* and *wild-type* were scored as combined results of two or more independently-derived extrachromosomal arrays with similar effects. *Pmyo-3::mab-5* is an integrated line. “Reeler” constructs contain the first 430 amino acids of SPON-1, while “SP::TSR-5” constructs contain the endogenous signal peptide (29 residues) followed by residues 431–819.

viable hypomorphic alleles *e2623* and *ju430ts* and the embryonic lethal putative null *ju402* to analyze AQR and PQR migration (Woo *et al.* 2008) (Figure 5A). Both hypomorphic mutants displayed AQR and PQR migration defects (Figure 5, B–D). *spn-1(ju402)* animals with wild-type maternal contribution (M^+) displayed the paralyzed, arrested at twofold-stage-of-elongation characteristic of BWM defects. Despite elongation arrest at the twofold stage, many embryos still hatched and displayed AQR and PQR migration (Figure 5E). Arrested *ju402* L1 larvae showed AQR and PQR migration defects (45 and 60%, respectively), with directional migration defects observed for both (Figure 5, E–G). Combined with the effects in weaker hypomorphic *spn-1* mutants, these results show that SPON-1 function is required for the ability to migrate, as well as direction of migration in the A/P axis.

SPON-1 can act in BWMs to control Q descendant migration

spn-1(+) expression driven in all BWMs using the *myo-3* promoter rescued AQR and PQR defects of hypomorphic *e2623* and *ju430* mutants (Figure 6). It also rescued the lethality and AQR and PQR defects of the null *ju402* mutant (Figure 6). This suggests that SPON-1 can function in BWMs to control AQR and PQR migration. The *myo-3* promoter does not show the posterior BWM expression bias observed with the *spn-1* promoter (Figure 3), yet *Pmyo-3::spn-1* efficiently rescued directional AQR and PQR defects in *spn-1(ju402)*. This suggests that *spn-1* might play a permissive rather than instructive role in migration, but an instructive role cannot be excluded.

In a wild-type background, expression of SPON-1 in BWMs by *Pmyo-3::spn-1* caused weak but significant defects (Table 1), suggesting that ectopic SPON-1 expression might perturb

cell migration. While *Pspn-1::gfp* expression is not normally observed in the Q lineages (Figure 3), expression of *spn-1* in the Q neuroblasts using the Q cell-specific *Pegl-17* promoter (Branda and Stern 2000; Cordes *et al.* 2006) caused defects in AQR (3%) and PQR (19%) migration in a *wild-type* background (Figure 1 and Table 1). We used this transgenic construct to test which parts of the SPON-1 molecule can perturb AQR and PQR migration. Vertebrate F-spondin is cleaved, forming multiple fragments (Zisman *et al.* 2007). The fragment containing thrombospondin repeats (TSR) 1–4 binds to a lipoprotein receptor-related protein (LRP), which repels axons, while the TSR5–6 fragment and the Reeler fragment both serve as attractants to developing axons. Weak and variable defects were observed with both fragments (Table 1), suggesting that both the TSR repeats and the Reeler/Spondin domain might participate in perturbing AQR and PQR migration. The *C. elegans* LRP molecule LRP-1 was not required for the effects of full-length *spn-1* expression, as *lrp-1(ku156)* had no effect on AQR/PQR migration and did not modify the *Pegl-17::spn-1* phenotype (data not shown).

MAB-5 promotes *spn-1* expression in BWMs

spn-1 transcripts were over-represented in the transcriptome of *mab-5* gain-of-function animals, indicating that MAB-5 stimulates *spn-1* expression (Tamayo *et al.* 2013). Previous reports indicated that *Pspn-1::gfp* was expressed in BWM cells (Woo *et al.* 2008). We analyzed *Pspn-1::gfp* expression at the time when the Q descendants are beginning their migrations in early L1 larvae 4–4.5 hr posthatching. Expression was observed in posterior BWM cells (Figure 3), but not in the Q cells as determined by the Q cell-specific marker *rdvIs1 (Pegl-17::mCherry)* (Branda and Stern 2000; Ou *et al.* 2010) (Figure 3). *Pspn-1::gfp* expression was in BWM cells adjacent to the Q neuroblasts, with expression

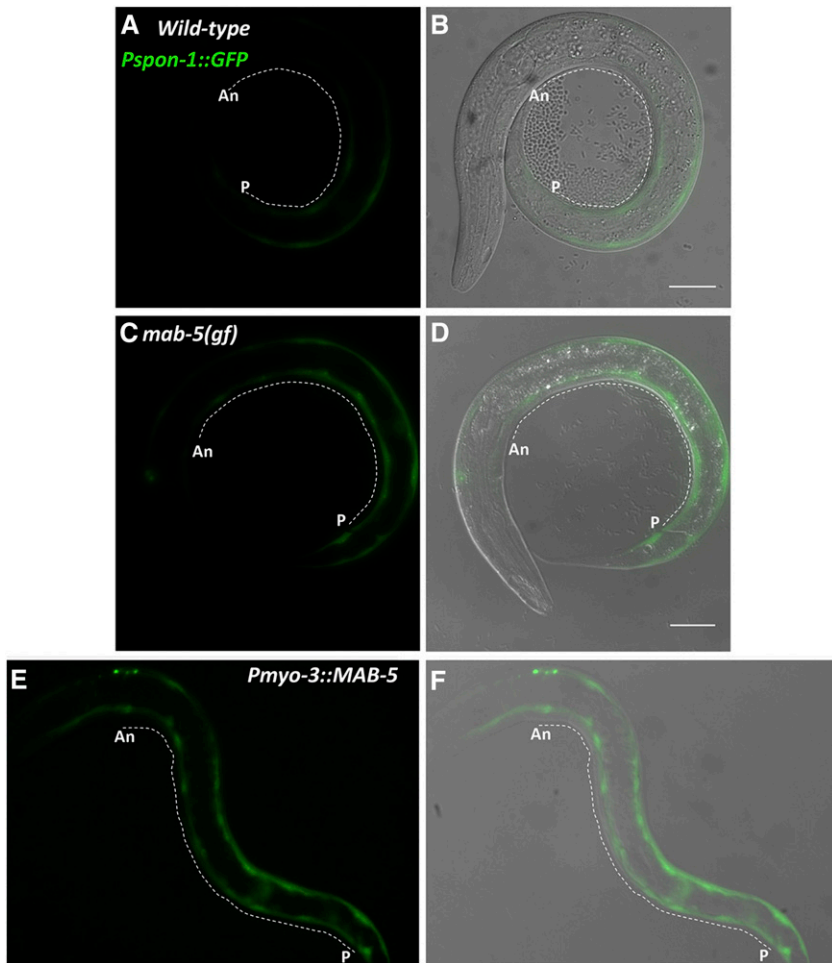


Figure 7 *Pspan-1::gfp* expression in *mab-5* gain of function. Fluorescent micrographs of *Pspan-1::gfp*-expressing L1 larvae 4–4.5 hr posthatching. Fluorescent *Pspan-1::gfp* (A, C, and E) and merged DIC (B, D, and F) micrographs. Dashed lines indicate regions of BWM used in line scans for the analysis in Figure 6 (An, anterior near the posterior pharyngeal bulb; P, posterior near the anus) (see *Materials and Methods*). Bar, 10 μ m.

extending posteriorly to the tail, but only a short distance anteriorly (Figure 3).

The gain-of-function *mab-5(e1751)* allele causes ectopic expression of *mab-5* in several tissues, including the QR lineage (Salser and Kenyon 1992; Salser *et al.* 1993). We found an increase in expression of the *Pspan-1::gfp* transgene in *mab-5(gof)* (Figure 7). While no expression was observed outside of BWMs, the extent of *Pspan-1::gfp* expression was increased anteriorly, with robust expression frequently present in anterior BWMs, sometimes reaching into the head (Figure 7, C and D). We quantified pixel intensity along line scans through the BWMs from anterior to posterior to quantify GFP intensity along the A/P axis (Figure 7 and Figure 8) (see *Materials and Methods*). *Wild-type* animals had little detectable expression along the first anterior 20%, after which GFP intensity rose steadily with the region of highest GFP intensity also correlated to the location of Q birth (Figure 3 and Figure 8A). *mab-5(gof)* had a significant increase in *Pspan-1::gfp* expression along the entire animal but still maintained the highest intensity around the Q cell birthplace (Figure 7, C and D and Figure 8A). These results indicate that *mab-5(gof)* increased *Pspan-1::gfp* in BWMs. This result is consistent with the RNA-seq results showing *span-1* overrepresentation in *mab-5(e1751)gof* animals (Tamayo *et al.*

2013). A whole-organism RNA-seq strategy was used in this study, so the sum of expression in all cells of the animal, including BWMs, was assayed. *mab-5* is expressed in QL and descendants as well as in other cells in the posterior, including posterior BWMs (Salser *et al.* 1993). We confirmed posterior BWM expression of the full-length *mab-5::gfp* transgene *mul516* in early L1 animals at the time when Q descendants begin migration (Hunter *et al.* 1999) (Figure 9).

We drove *mab-5* expression in all BWMs using the *myo-3* promoter. *Pmyo-3::mab-5* animals were grossly misshapen and could not be reliably quantified with line scans. However, in early L1 larvae, *Pmyo-3::mab-5* caused uniform expression of *Pspan-1::gfp* in all BWM cells from head to tail (Figure 7, E and F). These results show that in the BWMs, MAB-5 can activate *Pspan-1::gfp* expression. Together with the previous RNA-seq results (Tamayo *et al.* 2013), these data suggest that MAB-5 drives endogenous *span-1* expression in posterior BWMs adjacent to the Q cells.

MAB-5 is not required for *span-1* expression in BWMs

Consistent with the previous RNA-seq study that showed no effect on *span-1* transcript levels in *mab-5(lof)*, two *lof* alleles, *mab-5(e1239)* and *mab-5(e2088)*, had generally the same *Pspan-1::gfp* expression pattern as *wild-type* (Figure 8B)

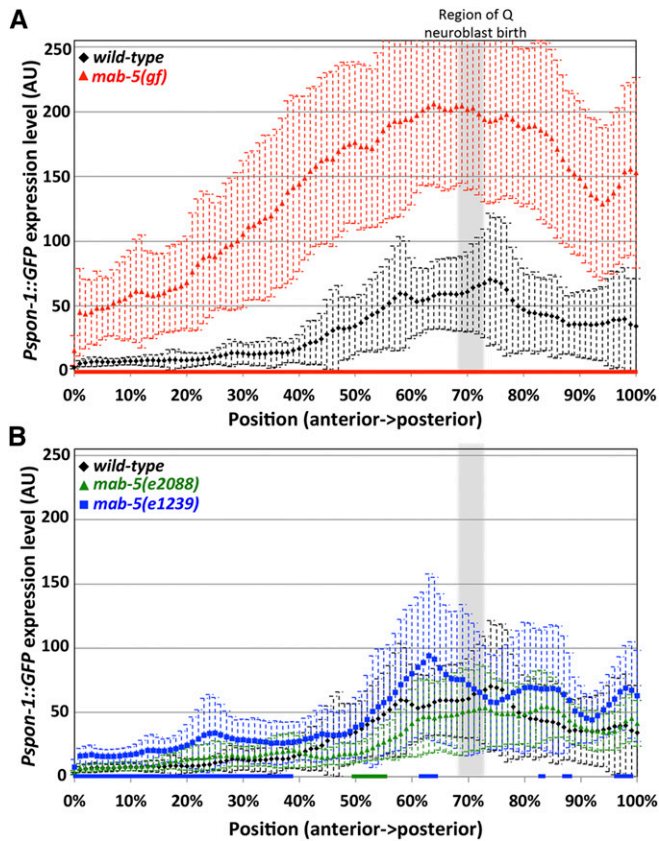


Figure 8 Quantification of *Pspn-1::gfp* intensity in BWMs. Graphs represent intensities of *Pspn-1::gfp* expression determined by line scans through BWM quadrants in L1 animals 4–4.5 hr posthatching (see *Materials and Methods*). The y-axis represents the intensity of GFP in arbitrary units (AU). The x-axis corresponds to position on the animal (0% is the posterior pharyngeal bulb, 100% is at the anus). The approximate region of Q neuroblast birth is shaded gray. Dashed error bars represent one standard deviation. Colored bars along the x-axis correspond to regions of significant difference compared to wild-type ($Q < 0.05$, multiple comparison corrected Student's *t*-test, $n = 40$ BWM quadrants) (two per animal, dorsal and ventral combined). (A) *mab-5(e1751)* gain of function. (B) *mab-5* putative null mutants *e2088* and *e1239*.

(Tamayo *et al.* 2013). Thus, while MAB-5 was sufficient to drive *spn-1* expression in BWMs, it was not required for *spn-1* expression.

Because *spn-1* expression persisted in *mab-5(lop)* animals, we speculated that other Hox genes *egl-5* and *lin-39* might act in parallel with *mab-5* to activate *spn-1* expression, especially given the parallel roles in AQR and PQR migration noted here (Figure 2). We tested *egl-5* single mutants, *mab-5 egl-5* double mutants, and a triple hox *lin-39 mab-5 egl-5* mutant on *Pspn-1::gfp* expression. None had any striking differences from *wild-type* animals (Figure 10A and Figure 11). However, despite triple Hox mutants' grossly misshapen bodies, they maintained a slightly increased expression pattern (Figure 11). An *hlh-1* binding site predicted by chromatin immunoprecipitation sequencing (ChIP-seq) is upstream of *spn-1* (Lei *et al.* 2010; Niu *et al.* 2011). *hlh-1* is the *C. elegans myoD* homolog and is required for BWM

formation (Chen *et al.* 1992, 1994). We tested the hypomorphic *hlh-1(cc561)* (Harfe *et al.* 1998) allele on *Pspn-1::gfp* expression and found no significant difference from *wild-type* (Figure 10B). Taken together, this suggests other factors might cooperate with MAB-5 to promote *spn-1* expression.

In double mutants of the *spn-1(e2623)* hypomorphic allele and *mab-5(null)* alleles *e2088* and *e1239*, AQR migration defects generally resembled *spn-1* alone (Table 2). Doubles with hypomorphic *mab-5* alleles *mu114* and *bx54* displayed significantly more AQR migration failure (Table 2). Misdirected PQR anterior migration also failed in double mutants, with hypomorphic *mab-5* alleles having the stronger effect (Table 2). The lack of strong genetic interaction between *mab-5* and *spn-1* loss-of-function mutations is consistent with our finding that *mab-5* is not required for *spn-1* expression. While we do not understand the nature of the genetic interactions with the *mab-5* hypomorphs, the results suggest that residual *mab-5* activity in *spn-1(e2623)* antagonizes anterior AQR and PQR migration.

SPON-1 suppresses *mab-5* gain of function

The gain-of-function *mab-5(e1751)* allele causes posterior migration of both AQR and PQR (Figure 12, A and B) (Chapman *et al.* 2008; Tamayo *et al.* 2013). Previously, SPON-1 was shown to be required for the full effect of *mab-5(gof)*, as *spn-1* knock-down with feeding RNAi partially suppressed posterior AQR migration in *mab-5(gof)* (Tamayo *et al.* 2013). The *spn-1 e2623* and *ju430ts* mutations also significantly suppressed posterior AQR migration to a similar extent in *mab-5* gain of function (Figure 12D): *mab-5(e1751)* displayed 78% of AQR neurons migrating posteriorly to the anus to the normal position of PQR, whereas *mab-5(e1751); spn-1(e2623)* displayed 56%, and *mab-5(e1751); spn-1(ju430ts)* at 15° had 57% of PQR posterior to the anus ($P < 0.05$) (Figure 12D).

We used transgenic RNAi of *spn-1* driven from the *myo-3*, *egl-17*, and *scm* promoters to knock down *spn-1* (Esposito *et al.* 2007; Sundararajan and Lundquist 2012). Alone, *Pmyo-3::spn-1(RNAi)* weakly affected AQR (1% defective) migration (Table 1). Because SPON-1 synthesis occurs in BWM and is required for embryogenesis, viable *Pmyo-3::spn-1(RNAi)* transgenes likely cause weak disruption of BWM-derived SPON-1 (*i.e.*, too weak to cause lethality). However, each RNAi construct suppressed *mab-5(gof)* (Figure 12, C and D). *mab-5(e1751)* rarely displayed AQR that were positioned anterior to the PDE neurons, the place of Q cell birth. In *mab-5(e1751); Pegl-17::spn-1(RNAi)* animals, AQR neurons were observed anterior to the PDE neuron (Figure 12C), illustrating suppression of *mab-5(e1751)gof*. In *C. elegans*, RNAi can spread from one cell to another via the double-stranded RNA channel SID-1, which has been used as a tool for cell-specific RNAi (Winston *et al.* 2002; Calixto *et al.* 2010). Suppression caused by the Q cell-specific *Pegl-17::spn-1(RNAi)* transgene was abolished by the *sid-1* mutation (Figure 12D). This suggests that suppression was due to RNAi spreading from the Q cells (likely to BWM), and that restriction of RNAi to the Q cells did not perturb *spn-1* function. In

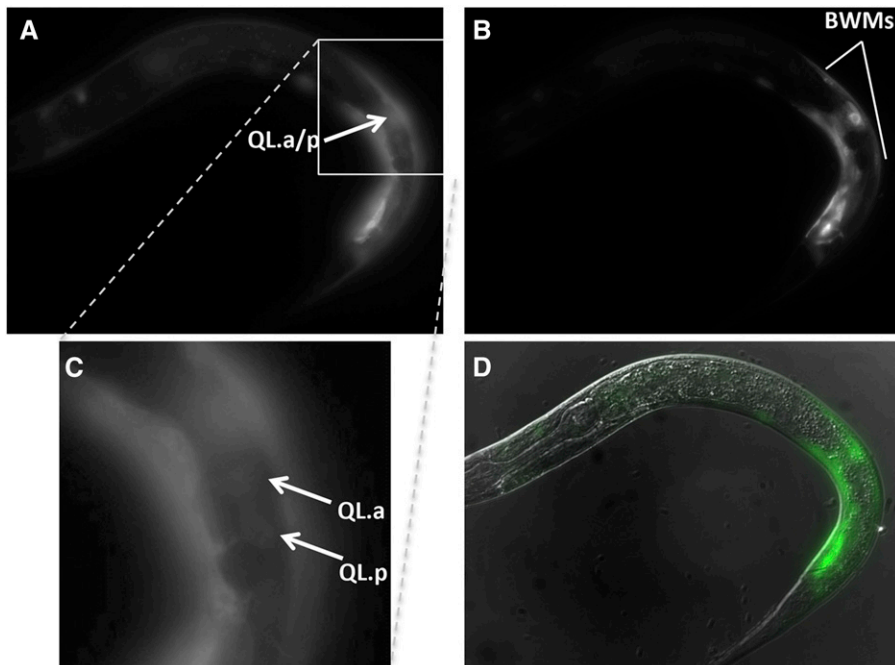


Figure 9 Expression of *mab-5::gfp (muls16)* in *wild-type* animals. Fluorescent micrographs of *muls16* animals 4–4.5 hr posthatching with left (A and C) and right (B) side of animal in focus. C is an enlargement of section in A to show faint expression in QL.a/p. (D) Merge of A and B and DIC. Bars, 5 μ m.

sum, these data indicate that *SPON-1*, likely from the BWMs, is partially required for posterior AQR migration observed in *mab-5(gof)*.

Discussion

Two main themes emerge from this work. First, our data indicate that the Hox factors *MAB-5*, *EGL-5*, and possibly *LIN-39* have nonautonomous parallel roles in Q descendant migrations. For *MAB-5*, this role is in contrast to the well-described autonomous function in QL. The nonautonomous roles of *LIN-39* and *MAB-5* are not apparent in single mutants due to redundancy, although *lin-39* mutants show some PQR migration defects. Second, this work shows that the secreted basement membrane molecule *SPON-1*, similar to vertebrate F-spondin, might be a transcriptional target of *MAB-5* in the BWM cells that nonautonomously influences Q cell migrations.

A nonautonomous role of *MAB-5* in Q descendant migration

Here we report a previously undescribed role of the Hox gene *mab-5* in the migration of the QR and QL descendants AQR and PQR. Previous studies showed that *MAB-5* autonomously regulates posterior migration of QL descendants (Salser and Kenyon 1992) and that *LIN-39* is autonomously required for anterior migration of QR descendants (Harris *et al.* 1996; Wang *et al.* 2013). We found that *lin-39 mab-5* double mutants displayed enhanced AQR anterior migration defects compared to *lin-39*, suggesting that *mab-5* and *lin-39* act in parallel pathways for anterior AQR migration. Furthermore, *lin-39* mutants alone displayed posterior PQR migration defects. *MAB-5* expression is not observed in the QR/AQR

lineage (Salser *et al.* 1993), and when expressed in this lineage, drives posterior migration. Additionally, *lin-39* is transiently expressed in QL/PQR lineage but is inhibited by *MAB-5* expression in this lineage when QL descendant migration occurs (Wang *et al.* 2013). These data suggest that *LIN-39* and *MAB-5* might have roles outside of the Q cells to regulate anterior AQR and posterior PQR migration. *lin-39* and *mab-5* are expressed in other posterior cells, including *mab-5* in posterior and midbody BWM (Salser *et al.* 1993; Clandinin *et al.* 1997; Maloof *et al.* 1999; Yang *et al.* 2005; Wagmaister *et al.* 2006a,b). Expression of *mab-5* in posterior BWMs rescued AQR migration defects in the *lin-39 mab-5* double mutant to resemble *lin-39* alone. It also rescued anterior migration defects of PQR in the *lin-39 mab-5* double. Of note, BWM expression of *mab-5* did not rescue the directional defects of PQR in the *lin-39 mab-5* double mutant, as all PQR still migrated anteriorly. Posterior migration of PQR is a cell-autonomous role of *mab-5*, and BWM expression of *mab-5* would not be expected to rescue directional defects. Together, these data point to a nonautonomous role of *MAB-5* in anterior AQR and PQR migration. The posterior PQR defects of *lin-39* could be due to a nonautonomous role or could be due to transient *lin-39* expression in the QL lineage (which is known to occur in *mab-5* mutants). This nonautonomous role for *MAB-5* on cell migration is in contrast to much of the work done with Hox genes that primarily has focused on cell-autonomous roles of these genes, but there is precedence for Hox genes in vertebrates noncell autonomously controlling axon guidance (Gavalas *et al.* 1997).

The *lin-39 mab-5 egl-5* triple mutant shows little or no Q descendant migration

egl-5 mutants displayed PQR migration defects and weak AQR migration defects, consistent with previous reports of

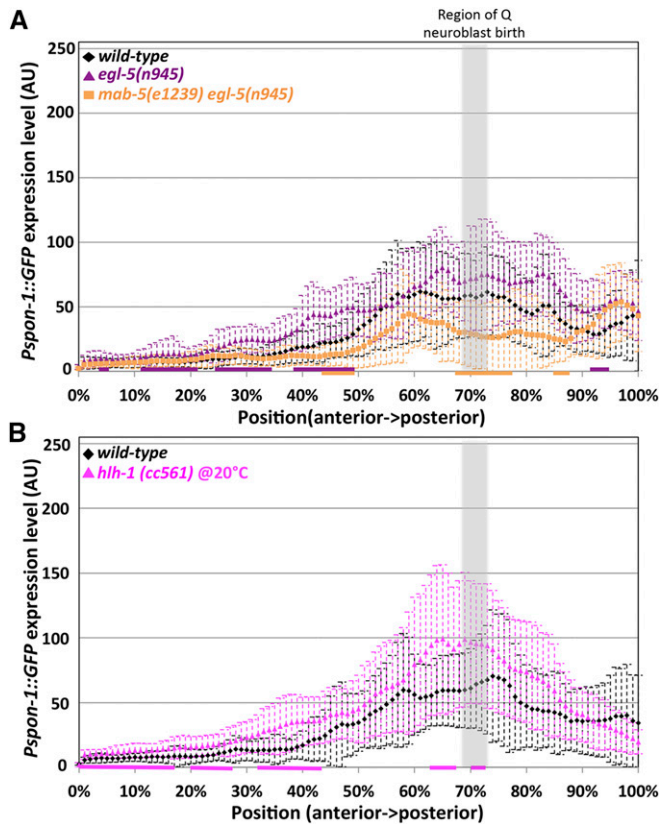


Figure 10 *egl-5* and *hlh-1* are not required for body wall expression of *Pspn-1::gfp*. Graphs represent intensities of *Pspn-1::gfp* expression determined by line scans through BWM quadrants in L1 animals 4–4.5 hr posthatching (see *Materials and Methods*). The y-axis represents the intensity of GFP in arbitrary units (AU). The x-axis corresponds to position on the animal (0% is the posterior pharyngeal bulb, 100% is at the anus). The approximate region of Q neuroblast birth is shaded gray. Dashed error bars represent one standard deviation. Colored bars along the x-axis correspond to regions of significant difference compared to wild type ($Q < 0.05$, multiple comparison corrected Student's *t*-test, $n = 40$ BWM quadrants) (two per animal, dorsal and ventral combined). (A) Wild-type, *egl-5*, and *mab-5 egl-5* double mutant. (B) Wild-type and *hlh-1(cc561)* hypomorphic allele.

Q lineage defects in *egl-5* (Chisholm 1991). Functional full-length *egl-5::gfp* expression was not observed in the Q lineages, and expressing EGL-5 specifically in posterior BWMs rescued *egl-5* defects. This suggests that *egl-5* might also non-autonomously regulate PQR migration, although expression in the Q lineages cannot be excluded as a possibility. The posterior PQR migration defects might be stronger in *egl-5* mutants, because the QL descendants migrate posteriorly through the region that expresses *egl-5*.

egl-5 did not enhance *mab-5* or *lin-39* defects, but did enhance AQR defects in the *lin-39 mab-5 egl-5* triple, which showed minimal migration of AQR and PQR away from the Q cell birthplace. This suggests that these three Hox genes act together to promote migration of the Q descendants, and in their absence, little or no anterior or posterior migration away from the Q cell birthplace occurs. In light of evidence presented here of a nonautonomous role of MAB-5, the

nearly complete lack of AQR and PQR migration in the *lin-39 egl-5 mab-5* triple is likely due to failure of both autonomous and nonautonomous roles of these molecules in AQR and PQR migration.

SPON-1/F-spondin controls Q descendant migration

Previously, RNA-seq identified *spn-1/F-spondin* as being positively regulated by MAB-5 in Q descendant migration (Tamayo *et al.* 2013). We found that mutations in *spn-1* caused AQR and PQR incomplete migration and directional defects. *spn-1* mutants partially suppressed *mab-5(gof)*, consistent with previous results using RNAi against *spn-1* (Tamayo *et al.* 2013). Restriction of *spn-1* RNAi to the Q lineages was insufficient for suppression, whereas RNAi in surrounding tissues and/or BWM resulted in suppression. This result suggests that *spn-1* acts nonautonomously in suppression of *mab-5(gof)*. This is consistent with *Pspn-1::gfp* expression, which we observed in posterior BWMs adjacent to the Q cells but not in the Q cells themselves.

spn-1 was expressed in posterior BWMs adjacent to the Q neuroblasts, and *spn-1* mutants displayed directional AQR and PQR migration defects. These results suggest that SPON-1 might provide directional guidance information for Q descendant migration. However, expression of SPON-1 from all BWM cells, from anterior to posterior, efficiently rescued AQR and PQR defects, a result not expected of a cue providing directional information. Therefore, SPON-1 might generally promote the ability of cells to migrate. The localized expression of *spn-1* adjacent to the Q cells in early L1 might represent a need for high levels of SPON-1 or newly synthesized SPON-1 to generally stimulate cell migration at that time. While *Pmyo-3::spn-1* does not provide localized expression, it might provide high levels of expression throughout larval development, when it is needed for cell migration. However, this does not explain the directional migration defects in *spn-1* mutants. *Pmyo-3::spn-1* expression caused weak AQR and PQR defects alone, consistent with a potential role in directed guidance. However, the preponderance of evidence suggests a permissive role of SPON-1 in cell migration, which differs from F-spondin in vertebrates, where it acts as a repellent to migrating neural crest cells (Debby-Brafman *et al.* 1999). However, there are also cases where F-spondin serves as an attractant and permissive signal to developing axons (Burstyn-Cohen *et al.* 1998, 1999; Zisman *et al.* 2007).

Increased levels of MAB-5 stimulates Pspn-1::gfp expression in BWM

We have shown that a *Pspn-1::gfp* transcriptional reporter was expressed at higher levels and more broadly in *mab-5(gof)*, consistent with previous RNA-seq showing that endogenous *spn-1* transcripts are over-represented in *mab-5(gof)* animals (Tamayo *et al.* 2013). Expression of *mab-5* in all BWMs resulted in robust *Pspn-1::gfp* expression in all BWMs, even those in the anterior. These experiments indicate that increased MAB-5 activity in the BWMs drives *Pspn-1::gfp* expression. A ChIP-seq

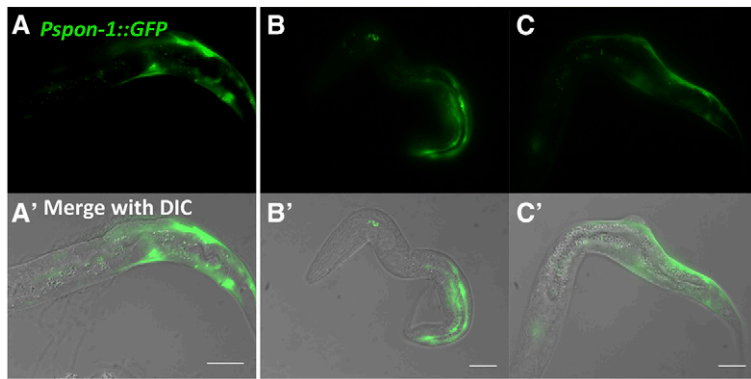
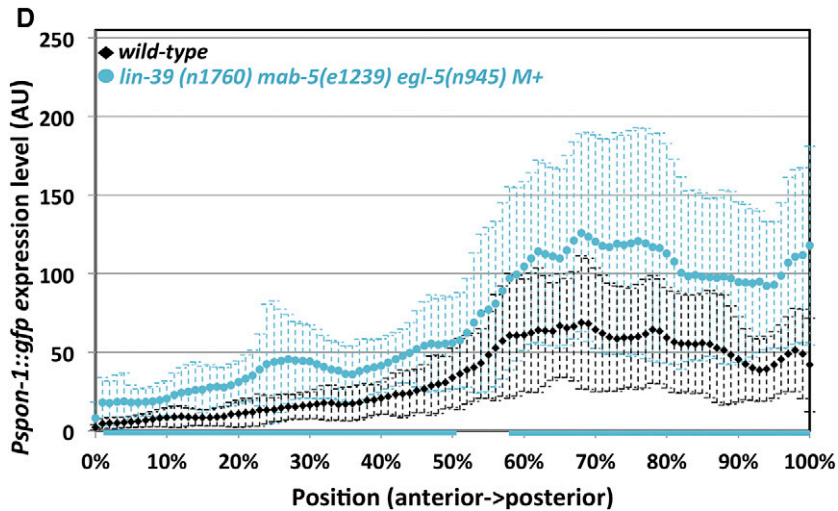


Figure 11 *Pspn-1::gfp* in *lin-39 mab-5 egl-5* triple mutant. Fluorescent micrographs (A–C) and merged DIC micrographs (A', B', and C') of three *lin-39(n1760) mab-5(e1239) egl-5(n945) M⁺* animals with *Pspn-1::gfp*. Animals are 4–4.5 hr posthatching. Bar, 10 μ M. Anterior is to the left, and dorsal is up. (D) Graphs representing intensity of *Pspn-1::gfp* expression in *lin-39 mab-5 egl-5 M⁺* as in Figure 8.



study using *MAB-5* (Niu *et al.* 2011) did not identify the *spn-1* locus as a potential *MAB-5* target. Thus, *MAB-5* might indirectly regulate *spn-1* expression in BWM. However, this ChIP-seq study was done with L3 larvae, long after Q migration, so any transient interaction at the *spn-1* promoter in L1 would have been missed. Because we only see increased *Pspn-1::gfp* levels in animals with overexpression of *mab-5*, it is possible that the increase in *Pspn-1::gfp* is due to aberrant binding to the *spn-1* promoter or other enhancers that may not occur in *wild-type* animals.

Complete loss of *SPON-1* function causes embryonic lethality, and *mab-5* mutants are not lethal, suggesting that *MAB-5* is not the only factor that regulates *spn-1* expression. Indeed, *mab-5(lof)* mutants did not affect *Pspn-1::gfp*, consistent with RNA-seq showing no effect of *mab-5(lof)* on *spn-1* transcript accumulation (Tamayo *et al.* 2013). The *lin-39 mab-5 egl-5* triple mutant also was able to express *Pspn-1::gfp* readily and may have increased *spn-1* expression. This indicates that neither *LIN-39* nor *EGL-5* cooperate with *MAB-5* in *Pspn-1::gfp* expression. The *spn-1* locus contains a predicted *hlh-1* binding region (Niu *et al.* 2011), but *hlh-1* also did not influence *spn-1* expression. While *MAB-5* is sufficient to drive *spn-1* expression, other factors might be required redundantly with *mab-5* in normal *spn-1* expression. Furthermore, *LIN-39* and *EGL-5* might be required for the

expression of factors that act in parallel to factors regulated by *mab-5* (e.g., *spn-1*). This redundancy could be in the same cell or in distinct cells, each expressing factors that influence AQR and PQR migration.

In addition to the well-characterized cell-autonomous function of *LIN-39* and *MAB-5* in Q migration, we find possible roles outside of the Q lineage to promote migration, roles that have been masked by redundancy of function of these

Table 2 *mab-5; spn-1* double mutant analysis

Genotype	AQR position (%)						PQR position (%)					
	1	2	3	4	5	N	1	2	3	4	5	N
<i>spn-1(e2623)</i>	98	1	1	0	0	158	0	1	0	1	98	159
<i>mab-5(e2088)</i>	100	0	0	0	0	249	96	2	1	0	1	249
<i>mab-5(e2088); spn-1(e2623)</i>	100	0	0	0	0	146	87	9	2	2	0	249
<i>mab-5(e1239)</i>	99	1	0	0	0	283	99	1	0	0	0	283
<i>mab-5(e1239); spn-1(e2623)</i>	97	2	0	0	1	316	92	3	3	1	1	316
<i>mab-5(bx54)</i>	100	0	0	0	0	161	86	11	2	1	0	161
<i>mab-5(bx54); spn-1(e2623)</i>	88*	7	5	1	0	176	80	13	5	1	2	176
<i>mab-5(mu114)</i>	100	0	0	0	0	202	83	11	4	0	1	202
<i>mab-5(mu114); spn-1(e2623)</i>	89*	9	0	0	0	226	72	20	7	0	0	225

* $P < 0.05$ compared to corresponding additive effect (not tested for PQR).

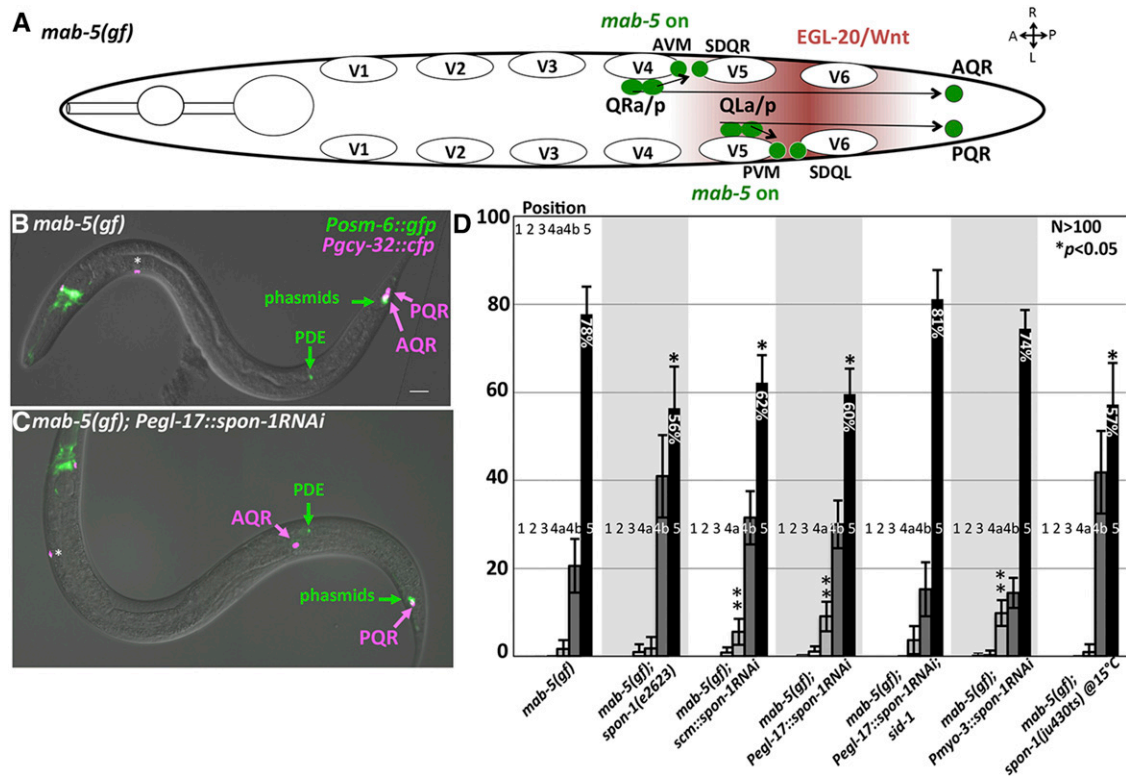


Figure 12 Suppression of *mab-5(gof)* by *spon-1*. (A) Diagram of Q descendant migration in *mab-5(e1751)* gain-of-function mutants as described in Figure 1A. *mab-5* is ectopically expressed in QR lineages, causing its descendants including AQR to migrate posteriorly. (B and C) Merged DIC and fluorescent micrographs of *mab-5(gof)* animals. *Posm-6::gfp* marks the PDE neuron, which serves as a landmark for Q birth position. The asterisk indicates an unidentified cell body present in *mab-5(gof)*, but not *wild type*, that expresses *Pgcy-32::cfp*. (D) Quantification of AQR position in *mab-5(e1751)gof* mutants alone and in double mutant combination (see Figure 2). Asterisks indicate a significant ($P < 0.05$, Fisher's exact test) reduction in the percentage of AQR residing in position 5 compared to *mab-5(gof)*. Double asterisk refers to genotypes with a significant increase in anterior migration (position 4a or more anterior) compared to *mab-5(gof)*. The locations 4a and 4b refer to location within position 4, with 4a anterior to PDE, and 4b posterior to PDE. Error bars represent 2× standard error of the proportion. *Pscm* and *Pegl-17 spon-1 RNAi* genotypes represent a combination of two independently derived transgenic lines with similar effects, and the *Pmyo-3* line represents combined results of three independent transgenic lines with similar effects.

molecules. We show evidence for a novel nonautonomous role of the Hox gene *mab-5* in Q migrations. *lin-39*, *mab-5*, and *egl-5* have distinct expression patterns, yet appear to have overlapping functions in promoting Q lineage migrations. We speculate that LIN-39, MAB-5, and EGL-5 pattern the posterior region of the animal for use as a substrate for Q migrations (a nonautonomous role), and that LIN-39 and MAB-5 control the response of the Q descendants to that posterior pattern (an autonomous role). Our data indicate that secreted basement membrane molecule SPON-1/F-spondin might be a target of MAB-5 in BWM and is important for Q descendant migration. In the absence of *lin-39*, *mab-5*, and *egl-5*, very little Q descendant migration away from the Q cell birthplace occurs, suggesting multiple and parallel pathways are regulated by these Hox factors in Q migrations.

Acknowledgments

We thank Eric Struckhoff for technical assistance; Andrew Chisholm and the *Caenorhabditis* Genetics Center, funded by National Institutes of Health (NIH) Office of Research Infrastructure Programs (P40-OD010440) for strains; and the

Lundquist and Ackley labs for helpful discussions. A.M.M. was a University of Kansas Undergraduate Research Award recipient and M.P.J. was supported by the Madison and Lila Self Graduate Fellowship Program at the University of Kansas. This work was funded by NIH grants R01-NS040945 and R21-NS070417 to E.A.L. and the Kansas Infrastructure Network of Biomedical Research Excellence (NIH grant P20-GM103418).

Literature Cited

- Arenkiel, B. R., P. Tvrdik, G. O. Gaufo, and M. R. Capecchi, 2004 Hoxb1 functions in both motoneurons and in tissues of the periphery to establish and maintain the proper neuronal circuitry. *Genes Dev.* 18: 1539–1552.
- Branda, C. S., and M. J. Stern, 2000 Mechanisms controlling sex myoblast migration in *Caenorhabditis elegans* hermaphrodites. *Dev. Biol.* 226: 137–151.
- Brenner, S., 1974 The genetics of *Caenorhabditis elegans*. *Genetics* 77: 71–94.
- Burstyn-Cohen, T., A. Frumkin, Y. T. Xu, S. S. Scherer, and A. Klar, 1998 Accumulation of F-spondin in injured peripheral nerve promotes the outgrowth of sensory axons. *J. Neurosci.* 18: 8875–8885.
- Burstyn-Cohen, T., V. Tzarfaty, A. Frumkin, Y. Feinstein, E. Stoeckli *et al.*, 1999 F-Spondin is required for accurate

- pathfinding of commissural axons at the floor plate. *Neuron* 23: 233–246.
- Calixto, A., D. Chelur, I. Topalidou, X. Chen, and M. Chalfie, 2010 Enhanced neuronal RNAi in *C. elegans* using SID-1. *Nat. Methods* 7: 554–559.
- Chalfie, M., J. N. Thomson, and J. E. Sulston, 1983 Induction of neuronal branching in *Caenorhabditis elegans*. *Science* 221: 61–63.
- Chapman, J. O., H. Li, and E. A. Lundquist, 2008 The MIG-15 NIK kinase acts cell-autonomously in neuroblast polarization and migration in *C. elegans*. *Dev. Biol.* 324: 245–257.
- Chen, L., M. Krause, B. Draper, H. Weintraub, and A. Fire, 1992 Body-wall muscle formation in *Caenorhabditis elegans* embryos that lack the MyoD homolog *hlh-1*. *Science* 256: 240–243.
- Chen, L., M. Krause, M. Sepanski, and A. Fire, 1994 The *Caenorhabditis elegans* MYOD homologue *HLH-1* is essential for proper muscle function and complete morphogenesis. *Development* 120: 1631–1641.
- Chisholm, A., 1991 Control of cell fate in the tail region of *C. elegans* by the gene *egl-5*. *Development* 111: 921–932.
- Clandinin, T. R., W. S. Katz, and P. W. Sternberg, 1997 *Caenorhabditis elegans* HOM-C genes regulate the response of vulval precursor cells to inductive signal. *Dev. Biol.* 182: 150–161.
- Clark, S. G., A. D. Chisholm, and H. R. Horvitz, 1993 Control of cell fates in the central body region of *C. elegans* by the homeobox gene *lin-39*. *Cell* 74: 43–55.
- Cordes, S., C. A. Frank, and G. Garriga, 2006 The *C. elegans* MELK ortholog PIG-1 regulates cell size asymmetry and daughter cell fate in asymmetric neuroblast divisions. *Development* 133: 2747–2756.
- Cowing, D. W., and C. Kenyon, 1992 Expression of the homeotic gene *mab-5* during *Caenorhabditis elegans* embryogenesis. *Development* 116: 481–490.
- Debby-Brafman, A., T. Burstyn-Cohen, A. Klar, and C. Kalcheim, 1999 F-Spondin, expressed in somite regions avoided by neural crest cells, mediates inhibition of distinct somite domains to neural crest migration. *Neuron* 22: 475–488.
- Desai, C., and H. R. Horvitz, 1989 *Caenorhabditis elegans* mutants defective in the functioning of the motor neurons responsible for egg laying. *Genetics* 121: 703–721.
- Dyer, J. O., R. S. Demarco, and E. A. Lundquist, 2010 Distinct roles of Rac GTPases and the UNC-73/Trio and PIX-1 Rac GTP exchange factors in neuroblast protrusion and migration in *C. elegans*. *Small GTPases* 1: 44–61.
- Esposito, G., E. Di Schiavi, C. Bergamasco, and P. Bazzicalupo, 2007 Efficient and cell specific knock-down of gene function in targeted *C. elegans* neurons. *Gene* 395: 170–176.
- Ferreira, H. B., Y. Zhang, C. Zhao, and S. W. Emmons, 1999 Patterning of *Caenorhabditis elegans* posterior structures by the Abdominal-B homolog, *egl-5*. *Dev. Biol.* 207: 215–228.
- Gavalas, A., M. Davenne, A. Lumsden, P. Chambon, and F. M. Rijli, 1997 Role of *Hoxa-2* in axon pathfinding and rostral hindbrain patterning. *Development* 124: 3693–3702.
- Hafez, D. M., J. Y. Huang, J. C. Richardson, E. Masliah, D. A. Peterson *et al.*, 2012 F-spondin gene transfer improves memory performance and reduces amyloid-beta levels in mice. *Neuroscience* 223: 465–472.
- Harfe, B. D., C. S. Branda, M. Krause, M. J. Stern, and A. Fire, 1998 MyoD and the specification of muscle and non-muscle fates during postembryonic development of the *C. elegans* mesoderm. *Development* 125: 2479–2488.
- Harris, J., L. Honigberg, N. Robinson, and C. Kenyon, 1996 Neuronal cell migration in *C. elegans*: regulation of Hox gene expression and cell position. *Development* 122: 3117–3131.
- Higashijima, S., A. Nose, G. Eguchi, Y. Hotta, and H. Okamoto, 1997 Mindin/F-spondin family: novel ECM proteins expressed in the zebrafish embryonic axis. *Dev. Biol.* 192: 211–227.
- Ho, A., and T. C. Sudhof, 2004 Binding of F-spondin to amyloid-beta precursor protein: a candidate amyloid-beta precursor protein ligand that modulates amyloid-beta precursor protein cleavage. *Proc. Natl. Acad. Sci. USA* 101: 2548–2553.
- Hoe, H. S., D. Wessner, U. Beffert, A. G. Becker, Y. Matsuoka *et al.*, 2005 F-spondin interaction with the apolipoprotein E receptor ApoEr2 affects processing of amyloid precursor protein. *Mol. Cell. Biol.* 25: 9259–9268.
- Honigberg, L., and C. Kenyon, 2000 Establishment of left/right asymmetry in neuroblast migration by UNC-40/DCC, UNC-73/Trio and DPY-19 proteins in *C. elegans*. *Development* 127: 4655–4668.
- Hu, H., N. Xin, J. Liu, M. Liu, Z. Wang *et al.*, 2016 Characterization of F-spondin in Japanese flounder (*Paralichthys olivaceus*) and its role in the nervous system development of teleosts. *Gene* 575: 623–631.
- Hunter, C. P., J. M. Harris, J. N. Maloof, and C. Kenyon, 1999 Hox gene expression in a single *Caenorhabditis elegans* cell is regulated by a caudal homolog and intercellular signals that inhibit wnt signaling. *Development* 126: 805–814.
- Ji, N., T. C. Middelkoop, R. A. Mentink, M. C. Betist, S. Tonegawa *et al.*, 2013 Feedback control of gene expression variability in the *Caenorhabditis elegans* Wnt pathway. *Cell* 155: 869–880.
- Josephson, M. P., Y. Chai, G. Ou, and E. A. Lundquist, 2016 EGL-20/Wnt and MAB-5/Hox act sequentially to inhibit anterior migration of neuroblasts in *C. elegans*. *PLoS One* 11: e0148658.
- Kalis, A. K., D. U. Kissiov, E. S. Kolenbrander, Z. Palchick, S. Raghavan *et al.*, 2014 Patterning of sexually dimorphic neurogenesis in the *Caenorhabditis elegans* ventral cord by Hox and TALE homeodomain transcription factors. *Dev. Dyn.* 243: 159–171.
- Kenyon, C., 1986 A gene involved in the development of the posterior body region of *C. elegans*. *Cell* 46: 477–487.
- Klar, A., M. Baldassare, and T. M. Jessell, 1992 F-spondin: a gene expressed at high levels in the floor plate encodes a secreted protein that promotes neural cell adhesion and neurite extension. *Cell* 69: 95–110.
- Korswagen, H. C., M. A. Herman, and H. C. Clevers, 2000 Distinct beta-catenins mediate adhesion and signalling functions in *C. elegans*. *Nature* 406: 527–532.
- Lei, H., T. Fukushige, W. Niu, M. Sarov, V. Reinke *et al.*, 2010 A widespread distribution of genomic CeMyoD binding sites revealed and cross validated by ChIP-Chip and ChIP-Seq techniques. *PLoS One* 5: e15898.
- Li, X., R. P. Kulkarni, R. J. Hill, and H. M. Chamberlin, 2009 HOM-C genes, Wnt signaling and axial patterning in the *C. elegans* posterior ventral epidermis. *Dev. Biol.* 332: 156–165.
- Maloof, J. N., J. Whangbo, J. M. Harris, G. D. Jongeward, and C. Kenyon, 1999 A Wnt signaling pathway controls hox gene expression and neuroblast migration in *C. elegans*. *Development* 126: 37–49.
- Mello, C., and A. Fire, 1995 DNA transformation. *Methods Cell Biol.* 48: 451–482.
- Mentink, R. A., T. C. Middelkoop, L. Rella, N. Ji, C. Y. Tang *et al.*, 2014 Cell intrinsic modulation of Wnt signaling controls neuroblast migration in *C. elegans*. *Dev. Cell* 31: 188–201.
- Middelkoop, T. C., and H. C. Korswagen, 2014 Development and migration of the *C. elegans* Q neuroblasts and their descendants (October 15, 2014). *WormBook*, ed. The *C. elegans* Research Community WormBook, doi/10.1895/wormbook.1.173.1, <http://www.wormbook.org>.
- Niu, W., Z. J. Lu, M. Zhong, M. Sarov, J. I. Murray *et al.*, 2011 Diverse transcription factor binding features revealed by genome-wide ChIP-seq in *C. elegans*. *Genome Res.* 21: 245–254.

- Ou, G., N. Stuurman, M. D'Ambrosio, and R. D. Vale, 2010 Polarized myosin produces unequal-size daughters during asymmetric cell division. *Science* 330: 677–680.
- Salser, S. J., and C. Kenyon, 1992 Activation of a *C. elegans* Antennapedia homologue in migrating cells controls their direction of migration. *Nature* 355: 255–258.
- Salser, S. J., and C. Kenyon, 1996 A *C. elegans* Hox gene switches on, off, on and off again to regulate proliferation, differentiation and morphogenesis. *Development* 122: 1651–1661.
- Salser, S. J., C. M. Loer, and C. Kenyon, 1993 Multiple HOM-C gene interactions specify cell fates in the nematode central nervous system. *Genes Dev.* 7: 1714–1724.
- Shen, Z., X. Zhang, Y. Chai, Z. Zhu, P. Yi *et al.*, 2014 Conditional knockouts generated by engineered CRISPR-Cas9 endonuclease reveal the roles of coronin in *C. elegans* neural development. *Dev. Cell* 30: 625–636.
- Studer, M., A. Lumsden, L. Ariza-McNaughton, A. Bradley, and R. Krumlauf, 1996 Altered segmental identity and abnormal migration of motor neurons in mice lacking Hoxb-1. *Nature* 384: 630–634.
- Sulston, J. E., and H. R. Horvitz, 1977 Post-embryonic cell lineages of the nematode, *Caenorhabditis elegans*. *Dev. Biol.* 56: 110–156.
- Sundararajan, L., and E. A. Lundquist, 2012 Transmembrane proteins UNC-40/DCC, PTP-3/LAR, and MIG-21 control anterior-posterior neuroblast migration with left-right functional asymmetry in *Caenorhabditis elegans*. *Genetics* 192: 1373–1388.
- Sundararajan, L., M. L. Norris, and E. A. Lundquist, 2015 SDN-1/Syndecan acts in parallel to the transmembrane molecule MIG-13 to promote anterior neuroblast migration. *G3 (Bethesda)* 5: 1567–1574.
- Tamayo, J. V., M. Gujar, S. J. Macdonald, and E. A. Lundquist, 2013 Functional transcriptomic analysis of the role of MAB-5/Hox in Q neuroblast migration in *Caenorhabditis elegans*. *BMC Genomics* 14: 304.
- Tzarfaty-Majar, V., R. Lopez-Aleman, Y. Feinstein, L. Gombau, O. Goldshmidt *et al.*, 2001 Plasmin-mediated release of the guidance molecule F-spondin from the extracellular matrix. *J. Biol. Chem.* 276: 28233–28241.
- Van Auken, K., D. C. Weaver, L. G. Edgar, and W. B. Wood, 2000 *Caenorhabditis elegans* embryonic axial patterning requires two recently discovered posterior-group Hox genes. *Proc. Natl. Acad. Sci. USA* 97: 4499–4503.
- Wagmaister, J. A., J. E. Gleason, and D. M. Eisenmann, 2006a Transcriptional upregulation of the *C. elegans* Hox gene *lin-39* during vulval cell fate specification. *Mech. Dev.* 123: 135–150.
- Wagmaister, J. A., G. R. Miley, C. A. Morris, J. E. Gleason, L. M. Miller *et al.*, 2006b Identification of cis-regulatory elements from the *C. elegans* Hox gene *lin-39* required for embryonic expression and for regulation by the transcription factors LIN-1, LIN-31 and LIN-39. *Dev. Biol.* 297: 550–565.
- Wang, B. B., M. M. Muller-Immergluck, J. Austin, N. T. Robinson, A. Chisholm *et al.*, 1993 A homeotic gene cluster patterns the anteroposterior body axis of *C. elegans*. *Cell* 74: 29–42.
- Wang, X., F. Zhou, S. Lv, P. Yi, Z. Zhu *et al.*, 2013 Transmembrane protein MIG-13 links the Wnt signaling and Hox genes to the cell polarity in neuronal migration. *Proc. Natl. Acad. Sci. USA* 110: 11175–11180.
- Whangbo, J., and C. Kenyon, 1999 A Wnt signaling system that specifies two patterns of cell migration in *C. elegans*. *Mol. Cell* 4: 851–858.
- White, J. G., E. Southgate, J. N. Thomson, and S. Brenner, 1986 The structure of the nervous system of the nematode *Caenorhabditis elegans*. *Philos. Trans. R. Soc. Lond.* 314: 1–340.
- Winston, W. M., C. Molodowitch, and C. P. Hunter, 2002 Systemic RNAi in *C. elegans* requires the putative transmembrane protein SID-1. *Science* 295: 2456–2459.
- Woo, W. M., E. C. Berry, M. L. Hudson, R. E. Swale, A. Goncharov *et al.*, 2008 The *C. elegans* F-spondin family protein SPON-1 maintains cell adhesion in neural and non-neural tissues. *Development* 135: 2747–2756.
- Yang, L., M. Sym, and C. Kenyon, 2005 The roles of two *C. elegans* HOX co-factor orthologs in cell migration and vulva development. *Development* 132: 1413–1428.
- Zisman, S., K. Marom, O. Avraham, L. Rinsky-Halivni, U. Gai *et al.*, 2007 Proteolysis and membrane capture of F-spondin generates combinatorial guidance cues from a single molecule. *J. Cell Biol.* 178: 1237–1249.

Communicating editor: M. V. Sundaram